REPORT DOCUMENTATION PAGE

Form Approved OMB NO. 0704-0188

1. REPORT DATE (DD-MM-YYYY)	2. REPORT TYPE	3. DATES COVERED (From - To)
13-02-2008	Final Report	15-Mar-2004 - 14-Sep-2007

4. TITLE AND SUBTITLE
Dislocation Core and Cross Slip Properties in Metals and Intermetallics: Linking ab initio and continuum approaches

5a. CONTRACT NUMBER
W911NF-04-1-0058

5b. GRANT NUMBER

5c. PROGRAM ELEMENT NUMBER
611102

6. AUTHORS
Nicholas G. Kioussis

5d. PROJECT NUMBER

5e. TASK NUMBER

5f. WORK UNIT NUMBER

7. PERFORMING ORGANIZATION NAMES AND ADDRESSES
California State University - Northridge
The University Corporation, CSU, Northridge
18111 Nordhoff Street
Northridge, CA 91330 -8232

8. PERFORMING ORGANIZATION REPORT NUMBER

9. SPONSORING/MONITORING AGENCY NAME(S) AND ADDRESS(ES)
U.S. Army Research Office
P.O. Box 12211
Research Triangle Park, NC 27709-2211

10. SPONSOR/MONITOR'S ACRONYM(S)
ARO

11. SPONSOR/MONITOR'S REPORT NUMBER(S)
45815-PH-H.10

12. DISTRIBUTION AVAILIBILITY STATEMENT
Approved for Public Release; Distribution Unlimited

13. SUPPLEMENTARY NOTES
The views, opinions and/or findings contained in this report are those of the author(s) and should not contrued as an official Department of the Army position, policy or decision, unless so designated by other documentation.

14. ABSTRACT
13. ABSTRACT (Maximum 200 words)
1) Developed, tested, and implemented a novel concurrent multiscale approach which improves the coupling-quality between the quantum and the classical atomistic regions. This approach, which allows for the first time the study of the dislocation core structure and the effect of chemistry (impurities) on the dislocation core, was applied successfully to aluminum. 2) Developed and applied a novel sequential multiscale approach which couples ab initio and continuum approaches to study the dislocation core and cross-slip properties of nano-layered Cu-Ni multilayered thin films; and the effect of twinning in fcc

15. SUBJECT TERMS
multiscale modeling; disolcation core properties; spintronics

16. SECURITY CLASSIFICATION OF:			17. LIMITATION OF ABSTRACT	15. NUMBER OF PAGES	19a. NAME OF RESPONSIBLE PERSON
a. REPORT	b. ABSTRACT	c. THIS PAGE			Nicholas Kioussis
U	U	U	SAR		19b. TELEPHONE NUMBER 818-677-7733

Report Title

Dislocation Core and Cross Slip Properties in Metals and Intermetallics: Linking ab initio and continuum approaches

ABSTRACT

13. ABSTRACT (Maximum 200 words)
1) Developed, tested, and implemented a novel concurrent multiscale approach which improves the coupling-quality between the quantum and the classical atomistic regions. This approach, which allows for the first time the study of the dislocation core structure and the effect of chemistry (impurities) on the dislocation core, was applied successfully to aluminum. 2) Developed and applied a novel sequential multiscale approach which couples ab initio and continuum approaches to study the dislocation core and cross-slip properties of nano-layered Cu-Ni multilayered thin films; and the effect of twinning in fcc metals. 3) Studied the spin transport in magnetic tunnel junctions and its anomalous bias dependence; and 4) Studied the effect of electron-phonon interaction in strongly correlated electron clusters on the interplay between the Kondo and magnetic ordering effect.

List of papers submitted or published that acknowledge ARO support during this reporting period. List the papers, including journal references, in the following categories:

(a) Papers published in peer-reviewed journals (N/A for none)

1. An improved multiscale modeling approach for metals, Y. Liu, Gang Lu, Zhengzheng Chen, and Nicholas Kioussis, Model. and Simulation in Materials Science and Engineering, 15, 275 (2007).
2. Local Chemistry Effect on Dislocation Mobility: Dual Nature of Solutes, Z. Chen, N. Kioussis, and G. Lu, to be submitted to Phys. Rev. Lett. (February 2008).
3. N. M. Ghoniem and N. Kioussis, Hierarchial Models of Nanomechanics and Micromechanics, Chap. 64, Handbook of Theoretical Computational Nanotechnology, Ed. M. Rieth and W. Schommers, Vol. 1, pp. 1-97 (2005).
4. Non-singular descriptions of dislocation cores: a hybrid ab initio continuum approach, S. Banerjee, N. M. Ghoniem, G. Lu, N. Kioussis, Phil. Mag. B 87, 4131 – 4150 (2007).
5. Dislocation threading across Cu/Ni interface: A hybrid atomistic-continuum approach, M. Shehadeh, G. Lu, N. Kioussis, S. Banerjee, and N. Ghoniem, Phil. Mag. 87, 1513 (2007).
6. Multiplane-induced widening of stacking faults in fcc metals, M. Shehadeh, G. Lu, N. Kioussis, and N. Ghoniem, Appl. Phys. Lett. 91, 171905 (2007).
7. Evolution of Magnetism of Cr nanoclusters on Au (111) surface: First principles electronic structure calculations, H. Gotsis, N. Kioussis, and D. Papaconstantopoulos, , Phys. Rev. B. 73, 014436 (2006).
8. Spin-polarized current-induced torque in magnetic tunnel junctions, A. Kalitsov, I. Theodonis, N. Kioussis, M. Chshiev, and W. Bulter, J. Appl. Phys. 99, 08G501 (2006).

9. Anomalous Bias Dependence of spin torques in magnetic tunnel junctions, I. Theodonis, N. Kioussis, A. Kalitsov, M. Chshiev, and W. H. Butler, Phys. Rev. Lett. 97, 237205 (2006).
10. Spin transfer torque in double barrier magnetic tunnel junctions, I. Theodonis, A. Kalitsov, and N. Kioussis, J. Magn. and Magn. Mater. 310, 2043 (2007).
11. Enhancing spin-transfer torque through the proximity of quantum well states, I. Theodonis, A. Kalitsov, and N. Kioussis, Phys. Rev. B 76, 224406 (2007).
12. Electron-Electron versus Electron-Phonon Interactions in Anderson-Holstein Nanoclusters, C. Verdozzi and N. Kioussis, to be submitted to Phys. Rev. B (2008).

Number of Papers published in peer-reviewed journals: 11.00

(b) Papers published in non-peer-reviewed journals or in conference proceedings (N/A for none)

Number of Papers published in non peer-reviewed journals: 0.00

(c) Presentations

The Invited Presentations are:

1. Spin Transfer Torque in magnetic tunnel junctions, USC, Department of Physics, Seminar, January 2007.
2. Current-induced spin torque in magnetic tunnel junctions, UCLA, Department of Materials Science, Colloquium, February 2006.
3. Anomalous bias effect on spin transfer in tunnel junctions, CSU Long Beach, Department of Physics, Colloquium, October 2006.
4. Enhancement of spin torque in double-barrier magnetic tunnel junctions, International Conference of Magnetism, Kyoto, Japan, August 20-25, 2006.
5. Spin Torque in magnetic tunnel junctions, Moscow International Symposium on Magnetism, Moscow State University, June 25-30, 2005.
6. Tuning the magnetism in strongly-correlated electron nanoclusters, presented at the Third International Conference on Correlation Effects and Materials Properties, Kos, Greece, July 2004.
7. Electronic Structure of Defect Reactions in Hydrogen-bonded Ferroelectrics, presented at Simulations of Complex Materials, March Meeting APS, Austin, Texas, March 3-7, 2003.
8. Tuning the magnetism in strongly-correlated electron nanoclusters, presented at NATO Advanced Research Workshop on "Physics of Spin in Solids: Materials, Methods, and Applications", Baku, Azerbaijan, October 15-19 2003.

Number of Presentations: 8.00

Non Peer-Reviewed Conference Proceeding publications (other than abstracts):

Number of Non Peer-Reviewed Conference Proceeding publications (other than abstracts): 0

Peer-Reviewed Conference Proceeding publications (other than abstracts):

Number of Peer-Reviewed Conference Proceeding publications (other than abstracts): 0

(d) Manuscripts

1. Local Chemistry Effect on Dislocation Mobility: Dual Nature of Solutes, Z. Chen, N. Kioussis, and G. Lu, to be submitted to Phys. Rev. Lett. (February 2008).

2. Electron-Electron versus Electron-Phonon Interactions in Anderson-Holstein Nanoclusters, C. Verdozzi and N. Kioussis, to be submitted to Phys. Rev. B (2008).

Number of Manuscripts: 2.00

Number of Inventions:

Graduate Students

NAME	PERCENT_SUPPORTED
Ioannis Theodonis	0.20
Bemjamin Ramirez	0.10
FTE Equivalent:	**0.30**
Total Number:	**2**

Names of Post Doctorates

NAME	PERCENT_SUPPORTED
Yi Liu	1.00
Zhengzheng Chen	0.70
FTE Equivalent:	**1.70**
Total Number:	**2**

Names of Faculty Supported

NAME	PERCENT_SUPPORTED	National Academy Member
Nicholas Kioussis	0.50	No
FTE Equivalent:	**0.50**	
Total Number:	**1**	

Names of Under Graduate students supported

NAME	PERCENT_SUPPORTED
FTE Equivalent:	
Total Number:	

Student Metrics

This section only applies to graduating undergraduates supported by this agreement in this reporting period

The number of undergraduates funded by this agreement who graduated during this period:	0.00
The number of undergraduates funded by this agreement who graduated during this period with a degree in science, mathematics, engineering, or technology fields:.....	1.00
The number of undergraduates funded by your agreement who graduated during this period and will continue to pursue a graduate or Ph.D. degree in science, mathematics, engineering, or technology fields:.....	1.00
Number of graduating undergraduates who achieved a 3.5 GPA to 4.0 (4.0 max scale):	2.00
Number of graduating undergraduates funded by a DoD funded Center of Excellence grant for Education, Research and Engineering:	0.00
The number of undergraduates funded by your agreement who graduated during this period and intend to work for the Department of Defense	0.00
The number of undergraduates funded by your agreement who graduated during this period and will receive scholarships or fellowships for further studies in science, mathematics, engineering or technology fields:	1.00

Names of Personnel receiving masters degrees

NAME
Mayra Tovar
William Gembel
Total Number: 2

Names of personnel receiving PHDs

NAME
Ioannis Theodonis
Total Number: 1

Names of other research staff

NAME	PERCENT_SUPPORTED
FTE Equivalent:	
Total Number:	

Sub Contractors (DD882)

Inventions (DD882)

REPORT DOCUMENTATION PAGE

Form Approved
OMB NO. 0704-0188

1. AGENCY USE ONLY (Leave Blank)	2. REPORT DATE January 31, 2008	3. REPORT TYPE AND DATES COVERED FINAL: 5/2003-6/2007

4. TITLE AND SUBTITLE
Dislocation Core and Cross Slip Properties in Metals and Intermetallics: Linking ab initio and continuum approaches

5. FUNDING NUMBERS
W911NF-04-1-0058

6. AUTHOR(S)
Nicholas Kioussis

7. PERFORMING ORGANIZATION NAME(S) AND ADDRESS(ES)
Department of Physics, California State University Northridge, 18111 Nordhoff Street, Northridge, CA 91330-8268

8. PERFORMING ORGANIZATION REPORT NUMBER AMSRD-ACC-R 70-1t P-41226-PH

9. SPONSORING / MONITORING AGENCY NAME(S) AND ADDRESS(ES)
U. S. Army Research Office
P.O. Box 12211
Research Triangle Park, NC 27709-2211

10. SPONSORING / MONITORING AGENCY REPORT NUMBER

11. SUPPLEMENTARY NOTES
The views, opinions and/or findings contained in this report are those of the author(s) and should not be construed as an official Department of the Army position, policy or decision, unless so designated by other documentation.

12 a. DISTRIBUTION / AVAILABILITY STATEMENT
Approved for public release; distribution unlimited.

12 b. DISTRIBUTION CODE

13. ABSTRACT (Maximum 200 words)
1) Developed, tested, and implemented a novel concurrent multiscale approach which improves the coupling-quality between the quantum and the classical atomistic regions. This approach, which allows for the first time the study of the dislocation core structure and the effect of chemistry (impurities) on the dislocation core, was applied successfully to aluminum. 2) Developed and applied a novel sequential multiscale approach which couples *ab initio* and continuum approaches to study the dislocation core and cross-slip properties of nano-layered Cu-Ni *multilayered thin films;* and the effect of twinning in fcc metals. 3) Studied the spin transport in magnetic tunnel junctions and its anomalous bias dependence; and 4) Studied the effect of electron-phonon interaction in strongly correlated electron clusters on the interplay between the Kondo and magnetic ordering effect.

14. SUBJECT TERMS

15. NUMBER OF PAGES

16. PRICE CODE

17. SECURITY CLASSIFICATION OR REPORT	18. SECURITY CLASSIFICATION ON THIS PAGE	19. SECURITY CLASSIFICATION OF ABSTRACT	20. LIMITATION OF ABSTRACT
UNCLASSIFIED	**UNCLASSIFIED**	**UNCLASSIFIED**	**UL**

DISLOCATION CORE AND CROSS SLIP PROPERTIES IN METALS AND INTERMETALLICS: LINKING AB INITIO AND CONTINUUM APPROACHES

FINAL PROGRESS REPORT
APRIL 2003 – OCTOBER 2007

PRINCIPAL INVESTIGATOR: Prof. Nicholas Kioussis

US ARMY RESEARCH OFFICE

CONTRACT/GRANT NUMBER: W911NF-04-1-0058

INSTITUTION: California State University Northridge
Department of Physics
18111 Nordhoff Street
Northridge, CA 91330-8268

Block 1. Agency Use Only (Leave blank)

Block 2. Report Date. Full publication date including day, month, and year, if available (e.g. 1 Jan 88). Must cite at least year.

Block 3. Type of Report and Dates Covered. State whether report is interim, final, etc. If applicable enter inclusive report dates (e.g. 10 Jun 87 - 30 Jun 88).

Block 4. Title and Subtitle. A title is taken from the part of the report that provides the most meaningful and complete information. When a report is prepared in more than one volume, repeat the primary title, and volume number, and include subtitle for the specific volume. On classified documents enter the title classification in parentheses.

Block 5. Funding Numbers. To include contract and grant numbers; may include program element number(s) project number(s), task number(s), and work unit number(s). Use the following labels:

C - Contract	**PR** - Project
G - Grant	**TA** - Task
PE - Program Element	**WU** - Work Unit Accession No.

Block 6. Author(s). Name(s) of person(s) responsible for writing the report, performing the research, or credited with the content of the report. If editor or compiler, this should follow the name(s).

Block 7. Performing Organization Name(s) and Address(es). Self-explanatory.

Block 8. Performing Organization Report Number. Enter the unique alphanumeric report number(s) assigned by the organization performing the report.

Block 9. Sponsoring/Monitoring Agency Name(s) and Address(es) Self-explanatory.

Block 10. Sponsoring/Monitoring Agency Report Number. (*if known)*

Block 11. Supplementary Notes. Enter information not included elsewhere such as; prepared in cooperation with....; Trans. of...; To be published in.... When a report is revised, include a statement whether the new report supersedes or supplements the older report.

Block 12a. Distribution/Availability Statement. Denotes public availability or limitations. Cite any availability to the public. Enter additional limitations or special markings in all capitals (e.g. NORFORN, REL, ITAR).

- **DOD** - See DoDD 4230.25, "Distribution Statements on Technical Documents."
- **DOE** - See authorities.
- **NASA** - See Handbook NHB 2200.2.
- **NTIS** - Leave blank.

Block 12b. Distribution Code.

- **DOD** - Leave Blank
- **DOE** - Enter DOE distribution categories from the Standard Distribution for unclassified Scientific and Technical Reports
- **NASA** - Leave Blank.
- **NTIS** - Leave Blank.

Block 13. Abstract. Include a brief (*Maximum 200 words)* factual summary of the most significant information contained in the report.

Block 14. Subject Terms. Keywords or phrases identifying major subject in the report.

Block 15. Number of Pages. Enter the total number of pages.

Block 16. Price Code. Enter appropriate price code (NTIS *only*).

Block 17. - 19. Security Classifications. Self-explanatory. Enter U.S. Security Regulations (i.e., UNCLASSIFIED). If form contains classified information, stamp classification on the top and bottom of the page.

Block 20. Limitation of Abstract. This block must be completed to assign a limitation to the abstract. Enter either UL (Unlimited) or SAR (same as report). An entry in this block is necessary if the abstract is to be limited. If blank, the abstract is assumed to be unlimited.

REPORT DOCUMENTATION PAGE (SF298)
(Continuation Sheet)

SCIENTIFIC PROGRESS AND ACCOMPLISHMENTS

I. Aims

This research work is supported by the US Army Grant (W911NF-04-1-0058). During the March 2003 – November 2007 grant period the major part of our effort focused on the:

1. Development, testing, and implementation of a novel concurrent multiscale approach which improves the coupling-quality between the quantum and the classical atomistic regions. This approach, which allows the study of the dislocation core structure and the effect of chemistry (impurities) on the dislocation core, was applied successfully to aluminum, a prototypical fcc metal, and the effect of chemistry in Ta, a prototypical bcc metal.

2. Development, test, and implementation of a novel sequential multiscale approach which couples *ab initio* and continuum to study the dislocation core and cross-slip properties of nano-layered Cu-Ni *multilayered thin films.* This approach is different than current methods which employ empirical interatomic potentials for nanolaminates and allows the study of curved dislocations and dislocation loops. This method has also been applied to study the effect of twinning in fcc metals.

3. Study of spin transfer of torque in magnetic tunnel junctions (both single and double barrier) and the effect of the bias dependence. We predicted a novel anomalous bias dependence which has been recently confirmed by two experimental groups in Japan and Cornell University.

4. Study the effect of electron-phonon interaction on the interplay between the Kondo and magnetic ordering effect in strongly correlated electron clusters.

The scientific personnel involved in the research work is listed in Sec. III. The publications resulted from this research work during the 2003 - September 2007 period and are listed in the Publications section of the report (Sec. IV).

II. Results/significance

1. A Novel improved multiscale modeling approach for metals

The challenge in computational materials science and engineering is that real materials usually exhibit phenomena in which the small-length-scale degrees of freedom require an accurate, and hence computationally expensive treatment.[1] On the other hand, a coarser and less accurate treatment is adequate for the rest degrees of freedom. The length scales range from Angstroms to micrometers, spanning four orders of magnitude. Modeling this

range of length scales via computer simulation presents significant challenges, since computations are limited by a maximum number of degrees of freedom for reasonable memory requirements and simulation times. It is exactly the goal of multiscale approaches to seamlessly couple the several regions involved.[1-3]

In a concurrent simulation, the system is often partitioned into domains characterized by different scales and physics. The challenge of any concurrent approach lies in establishing a high-quality coupling between the regions which are treated by different computational methods. Choly *et al*. have recently put forward[2] a general concurrent method which couples density functional theory (DFT)-based quantum simulations to classical atomistic simulations based on the Embedded Atom Method (EAM) for metallic materials. Despite the apparent success of the concurrent approach of Choly *et al*,[2] non-negligible errors nonetheless exist across DFT/EAM boundary. More specifically, when the interaction energy between the quantum and classical regions is determined from an atomistic classical potential, the forces in the classical region are determined by the atomistic classical potential. On the other hand, the forces in the quantum region and on the boundary separating the two regions are determined by both the quantum and classical atomistic energetics, with the quantum energetics dominating well within this region. This mismatch in forces obtained from the classical method and the DFT calculation can in turn introduce substantial errors on the forces acting on the atoms at the boundary, and degrade the seamless coupling across the boundary.

In is the purpose of this work to develop an improvement of the coupling-quality between the quantum and the classical atomistic regions of the concurrent approach of Choly *et al*,[2] which reduces in turn the coupling errors of the original approach. Briefly stated, the forces in the boundary region are determined from the classical energetics rather than the quantum energetics. The improved method does not introduce any additional computational effort and is trivial to implement. We have demonstrated the effectiveness of the improved versus the original approach by carrying out a comparative study of bulk Al. In order to improve the quality-coupling between regions I and II, we propose the following simple correction to the original approach. A third region, referred to as the *boundary* region is introduced, as shown in Fig. 1, which consists of several layers of DFT boundary (B) atoms next to the DFT/EAM boundary. As shown in the manuscript, although the *boundary*-region atoms are included in the DFT cluster calculations of the energy in region I, their positions are actually determined by the EAM bulk calculations. Namely, the *boundary* atoms serve as a buffer to protect the inner DFT atoms (e.g., where the defect center lies) from being exposed to the fictitious surface at the boundary.

Furthermore, we have applied the improved method to compute the Peierls stress of an edge dislocation in Al. The computation of Peierls stress in Al represents a difficult task because of its extremely low value. Numerical uncertainties associated with the computational boundary conditions, underlying force laws and interpretation of the results can be comparable to the value of the Peierls stress itself. Consequently, there are large discrepancies in the theoretical/computational estimates of the Peierls stress in Al.[4,5] On the experimental side, the situation is not better - the two orders of magnitude discrepancy between the Peierls stress estimated from internal friction measurements and from mechanical testing has been tantalizing for decades. Since the present method is a combination of DFT calculation of the dislocation core and of EAM simulations of the long-range elastic field of the dislocation, it gives a more accurate estimate of the Peierls stress compared to direct atomistic simulations of the entire system. The publications resulted from this research work are listed as Refs. 1-4 in Sec. IV.

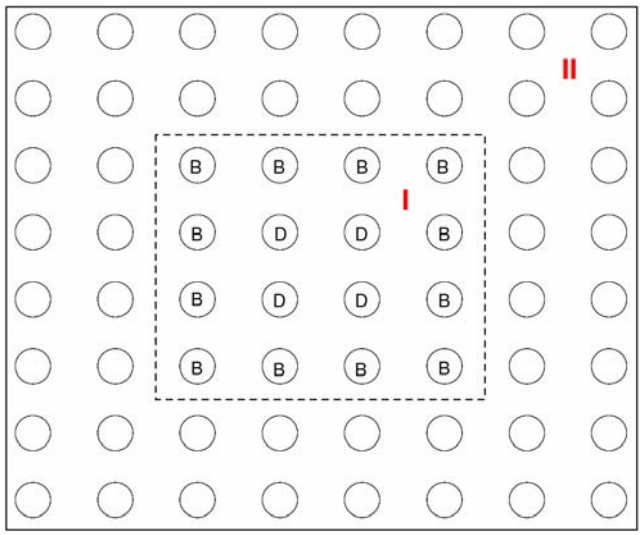

Figure 1 *Schematic of the test bulk system. The entire system is divided into regions I and II. The atoms marked by `B' are those atoms on the boundary between region I and II where the force correction is applied to. The atoms marked by `D' are defect core atoms*

Local Chemistry Effect on Dislocation Mobility: Dual Nature of Solutes

Dislocation interactions with impurities and solute atoms are an area of great practical importance, since solid solution hardening is a major means for altering the strength and plasticity of alloys. In most practical situations, dislocation behavior is considerably different in the realistically dirty materials, as opposed to the ideal pure ones, where dislocation mobility can vary by several orders of magnitude, depending on the nature of impurities, their concentration and local environment. Although continuum theory has provided considerable insight, our understanding of the physics of dislocation-solute interactions remains a challenging problem and atomistic simulations for predictive modeling of the non-linear effect of the dislocation core are still lacking. The major difficulty, in addition to those associated with length and time scales, is the lack of an accurate and computationally efficient description of interactions between moving dislocations and impurity atoms and clusters.

Much attention has been paid to alloys made of refractory metals, such as Nb, Mo, Ta, and W, which display high melting points. These alloys show excellent strength at elevated temperature and therefore have been found useful for high-temperature space and nuclear applications. It has been widely accepted that the low-temperature plasticity in bcc metals is governed by the a/2<111> screw dislocations, which due to the non-planar atomic core structure, have lower mobility compared to their edge segments.

Computations based on empirical interatomic potentials, tight-binding methods, and ab initio methods, produced very different results for the Peierls stress of a screw dislocation in Ta, indicating the inadequacy of interatomic potentials. In sharp contrast, the dislocation-solute interaction and in particular the effect of the alloying local environment remains an unexplored area thus far, due to the lack of reliable empirical potential for Ta and W interactions. This interaction can be divided into two general types depending on the characteristics of the short-range barrier. Barriers of the first type, e.g. solutes or groups of small precipitates are considered impenetrable and cannot be overcome by thermal fluctuation. In the second type, the short-range barrier is penetrable and the force-distance curves representing the interaction between solute atoms and dislocation line have both positive and negative components; the dislocation can overcome the solute atom by thermal fluctuation.

We have carried out a comprehensive study of the effects of chemistry and of solute local environment on the mobility (Peierls stress) and the Peierls potential in Ta-W alloys, using a novel concurrent multiscale approach,that we have recently developed. The results reveal

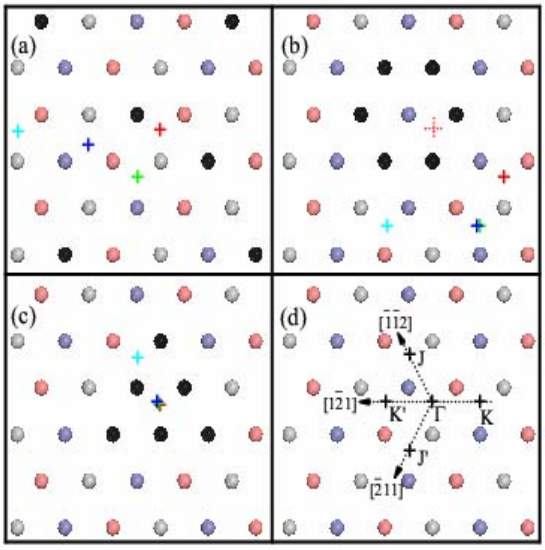

Fig. 2 *Screw dislocation slip paths under external stress for three local environments of W solutes denoted by black circles: (a) isolated solute atoms (ISA); and nano-clusters of (b) hexagonal shape (CSA-H) or of (c) triangular shape (CSA-T). The red, green, dark blue, and cyan crosses denote the position of the core center under 0.0, 1.0, 1.5, and 2.0 GPa, respectively. Circles of different color represent Ta atoms on three successive (111) planes. Panel (d) displays the special points and directions relevant for the Peierls potential surface in Fig. 2. G indicates the dislocation center in zero stress.*

that depending on the solute local environment (random solid solution or nano-clusters of different geometry and composition), the mobility and/or Peierls potential may exhibit a wide spectrum of unusual behavior: solid solution hardening or softening and it may even result in a collapse of the Peierls potential resulting in a spontaneous chemically-induced glide of the dislocation in the absence of externally applied stress.

In order to study the effect of solute local environmenton the mobility of the screw dislocation we have considered the cases of: 1) dilute random solid solutions where a given segment of dislocation line is only affected by an isolated solute atom (ISA) shown in Fig. 1a, and 2) solid solutions where small clusters of solute atoms of hexagonal shape (CSA-H) shown in Fig. 2b, or of triangular shape (CSA-T) interacting with a given dislocation line, shown in Fig. 2c. In all cases the W concentration is about 6 at.% and the W atoms are denoted with black circles. In all panels the red, green, dark blue, and light blue crosses denote the position of the dislocation core center under 0.0, 1.0, 1.5, and 2.0 GPa, respectively. Under 0.0 GPa the core center is at point Γ in panel (d) for the ISA and CSA-T cases, while it is unstable [dashed red cross in panel (b)] for the CSA-H case. Interestingly, in the latter case the dislocation center is repelled by the CSA-H and spontaneously moves to the position of the solid red cross indicating a precipitate-induced chemical stress. Under 1.0 GPa, both in the ISA and CSA-H cases the dislocation prefers to bypass the W sites and moves on the (011) plane. Upon increasing the stress to 1.5 GPa, the behavior changes dramatically: the dislocation in ISA continues to move, while it is pinned in CSA-H. The dislocation in CSA-H begins to move further under 1.8 GPa, as in the case in pure Ta. In sharp contrast to the other two cases, the dislocation core is pinned at Γ in the CSA-T case until one reaches 2.0 GPa stress, where the center moves on the 110 glide plane.

The calculated values of critical stress, σ_P, and polarization are listed in Table II, for the ISA, CSA-H, and CSA-T local environment. We find that isolated W atoms or W precipitates in the CSA-H local environment result in solid solution softening (SSS), while precipitates in the CSA-T produce solid solution hardening (SSH). Furthermore, in all cases W solid atoms have a small effect on polarization, indicating the absence of correlation between the polarization and the Peierls stress. Interestingly W solute atoms, independent of their local environment, do not change the core structure, in contrast to Cu precipitates in Fe. The underlying origin in electronic structure for the behavior of is that when the dislocation center lies in the vicinity

of W-rich local environment it requires the breaking of W-W and/or W-Ta strong bonds, compared to the Ta-Ta bonds, which are energetically unfavorable giving rise to a lower dislocation mobility as in the CSA-T configuration. However, the dislocation bypass the W solutes both in the ISA or CSA-H configurations. Thus, changes of the local solute chemical environment have a dramatic effect both on the slip paths and the mobility of the screw dislocation.

Closely related the Peierls stress is another measure of the lattice resistance to dislocation motion - the Peierls barrier. The Peierls barrier (per unit length of the dislocation line) is defined as the energy barrier that a straight dislocation must surmount in order to move to a neighboring lattice position - Peierls valley. A major challenge in dislocation modeling has been an accurate determination of the Peierls potential surface (PPS) and the role of impurities or solutes. Edagawa et al suggested that the dislocation motion in bcc metals can be viewed as 2D surface in the xy plane perpendicular to the direction of the Burgers vector Using the multiscale approach we have determined the PPS, by moving the dislocation center along different directions in Fig. 2(d). The PPS along the various <121> directions for pure Ta, and the ISA, CSA-T environments is shown in Fig. 3(a) and the corresponding CSA-H is shown in Fig. 3(b). We find that the Peierls barrier along the Γ–K' and Γ-J' are reduced compared to pure Ta, consistent with the results of Peierls stress in Table II. On the other hand, the CSA-H environment has a dramatic effect on the PPS on the (101) plane along the <121> direction, where the Peierls barrier between Γ and K is greatly reduced, consistent with the result that the dislocation glides spontaneously (under zero stress) to the position marked with the dashed cross in Fig. 1(b). Finally, for the ASC-T configuration, the barrier along [121] increases while that along [112] remains the same as in Ta. Thus, the dislocation first glides on the (110) plane, which is different from that in Ta.

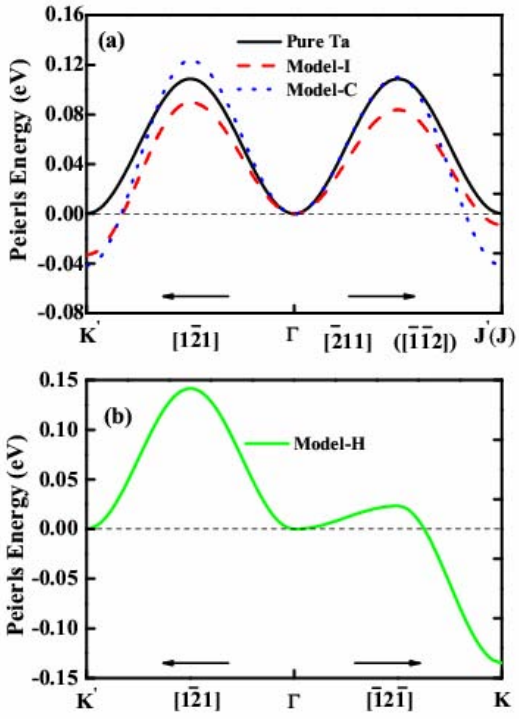

Figure 3 *Peierls potential surface along the various <121> directions in Fig. 1(d) for: (a) Pure Ta (black solid curve), the ISA environment (red dashed curve), and the CSA-T environment (blue dotted curve); and (b) for the CSA-H environment (green solid curve). The direction and special point in parenthesis in Fig. 2(a) correspond to the CSA-T environment.*

Table I *The Peierls stress (GPa) and polarization for: isolated solute atoms (ISA), nano-clusters of solute atoms of hexagonal shape (CSA-H) or of triangular shape (CSA-T), shown in Fig. 2.*

	ISA	CSA-H	CSA-T
σ_p	1.0	1.0	2.0
p	0.10	0.04	0.00

The publications resulted from this research work are listed as Refs. 1-4 in Sec. IV.

2. Dislocation core and cross-slip properties of nano-layered Cu-Ni multilayered thin films- A hybrid atomistic – continuum approach

The influence of interfaces on the mechanical properties of multiphase and polycrystalline materials is ubiquitous. The mechanical properties of an interface are determined, in large part, by the nature of the chemical bonding at the interface, which may be significantly different from that within either of the materials meeting at the interface. The variation of the Generalized stacking fault surface (GSFS) of the interface, the existence of misfit dislocations, and the lattice mismatch can act as barriers to dislocation motion and transmission across the interface. In recent years, there has been considerable interest in the mechanical and structural properties and the deformation mechanisms of metallic multilayer systems, which display remarkably high mechanical strength and hardness comparable to their theoretical strength.[6,7] It has been found experimentally that the hardness and ultimate tensile strength of nano-layered structures increases with decreasing bilayer thickness, in a relation analogous to the Hall-Petch behavior to some critical layer thickness. At smaller wavelengths, the hardness is seen to increase more rapidly, with Hall-Petch exponents on the order of unity or greater, to some peak stress value that is much greater than that attainable by traditional microstructures. Thus, multilayers composed of alternating layers made of metals such as Cu, Ni, Cr and Nb exhibit peak strengths on the order of few GPa at layer thickness of few nanometers, [6,7] compared to the yield strength values of few tens of MPa in bulk Cu, Ni, Cr and Nb.

The dramatic enhancement of multilayer strength has been generally attributed to the following factors: the mismatch in the elastic properties which results in image forces on the dislocation, the mismatch in the GSFS between incoming and outgoing planes which plays a major role in determining the core properties of the dislocation, the mismatch in the lattice parameters that leads to the generation of coherency stress across the interface, and the GSFS of the interface which may suppress or enhance the spreading of the dislocation core from the glide plane to the interface. Additionally, the existence of misfit dislocations affects the overall strength of multilayers as a result of their mutual interaction with glide dislocations. Molecular dynamics (MD) simulations have been used extensively to study different deformation mechanisms in bimaterials.[8,9] *Although MD simulations are very useful in revealing the atomistic mechanism for the strengthening effect in mulilayers, they suffer from the lack of reliable empirical potentials for treating interatomic interactions across the interface, especially when one considers new materials for which empirical interatomic potentials are not available.*

We have developed an extension of the Peierls-Nabarro model which integrates the atomistic nature from *ab initio* electronic structure calculations into the Parametric Dislocation Dynamics method. The GSFS provides a *two-dimensional representation* of the stacking fault energy at zero temperature.[10-12] Both coherent and incoherent interfaces are considered and the lattice resistance of dislocation motion is captured through the *ab initio*-determined GSFS. In this study, the core properties of a pure screw dislocation as it moves from Cu to Ni are investigated. We have also determined the effects of the GSFS of the interface on dislocation core spreading and on the transmission stress. Additionally, the effect of pre-existing misfit dislocation on interfacial strength and dislocation core spreading is investigated.

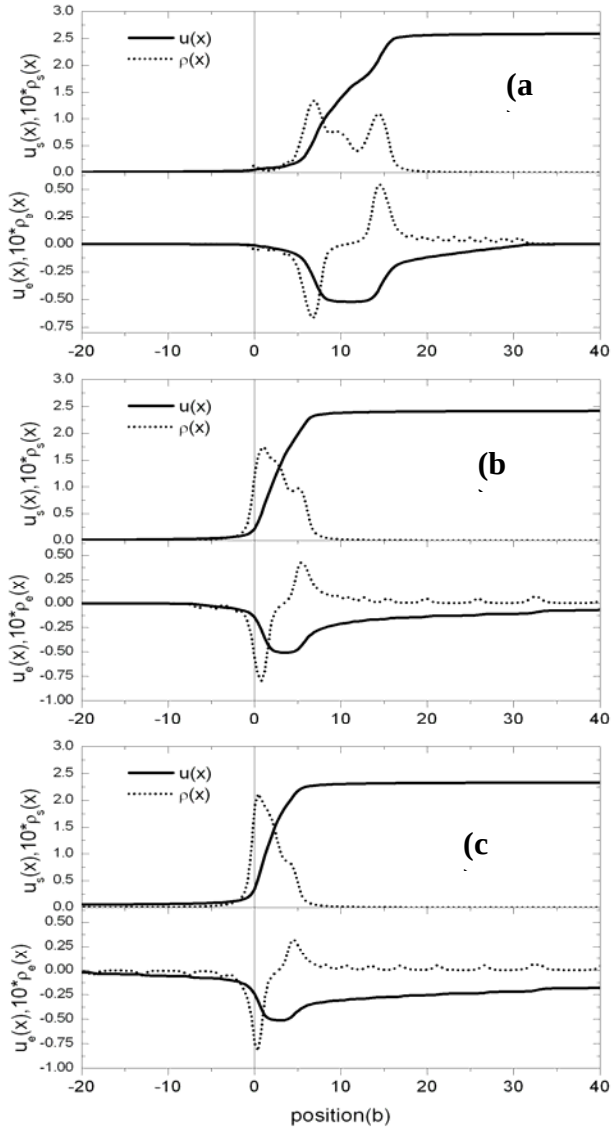

Figure 4 *The displacement u(x) and density ρ(x) profiles for the dislocation as it moves from Cu towards Ni. The GSFS of the interface is equal to the ab initio value* $\left(\gamma_{\text{int}} = \gamma_{\text{int}}^{ab}\right)$. *The profiles show the equilibrium positions of the dislocation at (a) 2.0 GPa, (b) 2.8 GPa and (c) 3.30 GPa. The continuous lines represent the screw or the edge displacements and the dotted lines represent the corresponding densities.*

Burgers vector density ρ(x) of the dislocation for three values of applied stress. The edge and screw Burgers vector density are defined by $\rho_e(x) = du_e/dx$, and $\rho_s(x) = du_s/dx$. Figure 4 shows the equilibrium edge and screw displacement and the corresponding dislocation density. The screw dislocation, originally placed in the soft material (x>0) is pushed towards the Cu/Ni interface. For relatively low values of applied stress (around 2.0 GPa), the dislocation core in Cu dissociates into two partials bounding a stacking fault with a separation distance of about 7b (figure 4a). As the external stress increases, the dislocation approaches the interface but remains dissociated. However; the dislocation core structure has changed significantly. First, the dislocation Burgers vector density accumulates on the leading partial at the expense of the trailing partial (figure 4 b,c). Second, the dislocation core constricts steadily and the two partials become significantly overlapped (figure 4c). Note, that the maximum value of the screw component of the displacement in Cu is 2.35 Å, while the Burgers vector of Cu is 2.6 Å. This reduction of Burgers vector is a result of the energetically favorable spreading of the core onto the interface. Our results suggest that the dislocation spreading process proceeds via the following mechanism: When the leading fractional dislocation reaches the vicinity of the interface it spreads on it, if it is

energetically favorable. As the external stress is increased, the trailing fractional dislocations follow and spread onto the interface. The spreading process continues until the interface can no longer accommodate additional slip. At the critical value of the applied stress, once the leading dislocation on the glide plane overcomes the interfacial barrier and is transmitted to the Ni crystal, the remaining fractional dislocations follow.

Figure 5 shows the critical transmission stress versus the ratio of γ_{int} with respect to its a*b initio* value for the cases of a non-slipping (rigid) and a slipping interface, with and without the edge component taken into account. The number in parenthesis indicates the percentage dislocation content on the interface for the case of slipping interface with the edge component taken into account. As expected, the critical transmission stress is independent of γ_{int} for the case of a rigid interface, and its value is higher when the edge component is neglected in the simulations. For the case of a slipping interface, when $\gamma_{int} < \gamma_{int}^{ab}$, the interface allows more dislocation content to spread from the glide plane to the interface. This in turn leads to a dramatic increase in the critical stress for transmission. For example, the critical stress is increased by a factor of three for $\gamma_{int} = 0.60\gamma_{int}^{ab}$, compared to the corresponding value at $\gamma_{int} = \gamma_{int}^{ab}$. On the other hand, when $\gamma_{int} > \gamma_{int}^{ab}$, the GSFS of the interface increases, the interfacial slipping becomes more difficult and the critical stress decreases more slowly saturating to a value of about 2.8 GPa. Thus, these results clearly demonstrate that the increase of transmission stress is directly related to the spreading process on the interface. Note, that the percentage of dislocation content on the interface increases from about 10% at $\gamma_{int} = 1.50\gamma_{int}^{ab}$ to 98% at $\gamma_{int} = 0.60\gamma_{int}^{ab}$. A similar trend of the critical transmission stress as a function of the interfacial energy barrier is also found for the case of slipping interface without taking into account the edge components (plain circles), but with higher values of critical stress. Our calculations show for the first time that the removal of the edge components results in dramatically different values for the transmission stress compared to those if the dissociation is included. The publications resulted from this research work are listed as Refs. 5-6 in Sec. IV.

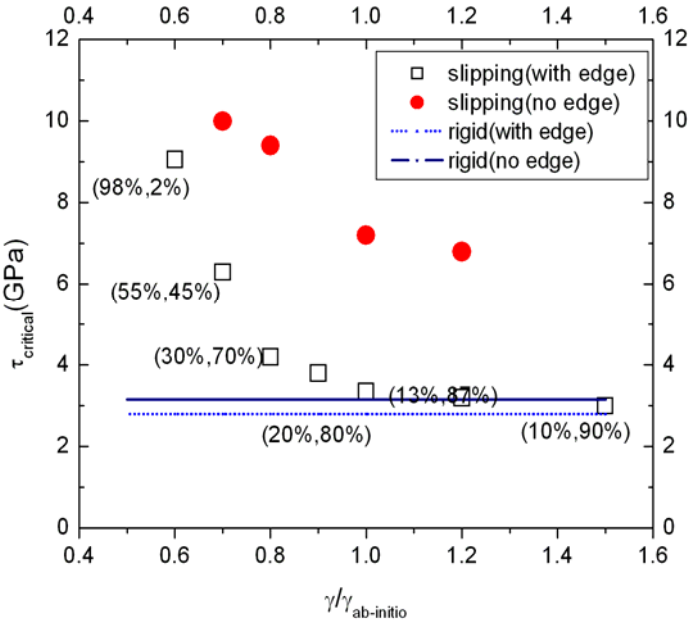

Figure 5. *The variation of the critical shear stress with the GSFS of the interface. Rigid interface does not accommodate core spreading and therefore it is not affected by the change in interfacial GSFS. The removal of the edge component leads to a significant increase in the transmission stress for the slipping interface case and minor increase for the rigid interface case.*

3. Anomalous Bias Dependence of Spin Torque in Magnetic Tunnel Junctions

When a spin-polarized current passes through a magnetic multilayer structure, whether spin valve or magnetic tunnel junction (MTJ), it can transfer spin angular momentum from one ferromagnetic electrode to another, and hence exert a torque on the magnetic moments of the electrodes.[13-16] At sufficiently high current densities, this spin transfer can stimulate spin-wave excitations and even reverse the magnetization of an individual domain. Current-induced magnetic switching (CIMS) has now been confirmed in numerous experiments both in spin valves[17] and more recently, in MTJs[18]. Thus, CIMS provides a powerful new tool for the study of spin transport in magnetic nanostrutures. In addition, it offers the intriguing possibility of manipulating high-density nonvolatile magnetic-device elements, such as magnetoresistive random access memory (MRAM), without applying cumbersome magnetic fields.[19] The effect of current-induced switching on the orientation of magnetic moments in magnetic heterostructures has recently attracted significant interest due to its potential applications to spin electronics, such as current-controlled magnetic memory elements.

While the fundamental physics underlying the spin transfer torque in spin valves has been extensively studied theoretically, its role in MTJs remains an unexplored area thus far, except for the pioneering work of Slonczewski, [13,15-16] who employed the free-electron model in the low bias regime. One of the most pressing needs is a comprehensive understanding of the bias dependence of the spin transfer torque in MTJs, which will be important for the development of MRAM that uses CIMS for writing the cell.

In this work, we investigated for the first time the effect of bias on the spin torques, parallel $T_{\parallel}$ and perpendicular $T_{\perp}$ to the interface, in MTJs, using tight-binding (TB) calculations and the non-equilibrium Keldysh formalism. We predict an anomalous bias dependence of the spin torque, contrary to the general consensus. We demonstrate first that depending on the exchange splitting, $T_{\parallel}$ may exhibit an unusual and interesting non-monotonic bias dependence: it may change sign *without a sign reversal in bias or current*, and in some cases it may even have a quadratic bias dependence. Second, both the TB calculations and a generalization of the equivalent circuit in Ref.16 using angular-dependent resistances, indicate that $T_{\parallel}$ satisfies an expression involving the difference in spin currents between the ferromagnetic (FM) and antiferromagnetic (AF) configurations. Third, the bias dependence for the spin current for the FM (AF) alignment is shown to have a linear (quadratic) bias dependence, whose origin lies in the symmetric (asymmetric) nature of the barrier. The interplay of the spin currents for the FM and AF configurations can lead to a rich behavior of the spin transfer torque on bias. Finally, we find that the bias dependence of $T_{\perp}$ is quadratic.

In Figure 6 we display the bias dependence of the parallel component of the *net* spin torque, $T_{\parallel}$, (curves associated with the left ordinate) for $\theta=\pi/2$ and for the same values of $\varepsilon_{\downarrow}$ (exchange splitting). The most striking and surprising feature of $T_{\parallel}$, is its non-monotonic bias dependence, which can vary from almost linear to purely quadratic behavior, depending on the exchange splitting Δ. The quadratic bias dependence of $\varepsilon_{\downarrow}$ =1.5eV persists even for small bias. Interestingly, for $\varepsilon_{\downarrow}$=2eV and 2.25eV, the spin torque *reverses its sign without a sign reversal in bias or current*. This anomalous bias behavior,

contrary to the general consensus, may have important practical implications, since it suggests that the CIMS in MTJ may not require reversal of the current.

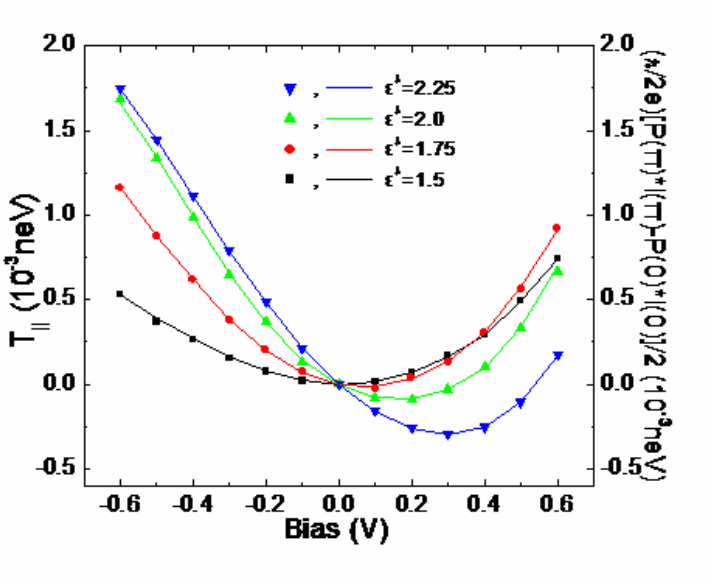

Figure 6 *Bias dependence of the parallel component of the net spin transfer torque per unit area, $T_{||}$, for q=p/2, and various values of $\varepsilon_{\downarrow}$. The curves (symbols) refer to the left- (right-) hand ordinate, respectively.*

In order to understand the underlying mechanism responsible for the bias-dependence of $T_{||}$, we have generalized the equivalent circuit for MTJ, using angular-dependent resistances, and have shown that $T_{||}$ satisfies the *universal* expression

$$T_{||}(\theta)=\frac{I^{(s)}(\pi)-I^{(s)}(0)}{2}\vec{M}_2\times(\vec{M}_1\times\vec{M}_2)=\frac{\hbar}{2e}\frac{P(\pi)I(\pi)-P(0)I(0)}{2}\vec{M}_2\times(\vec{M}_1\times\vec{M}_2)$$

where, $I^{(s)}(\pi)=\frac{\hbar}{2e}\left(I^{(\uparrow)}(\pi)-I^{(\downarrow)}(\pi)\right)$ and $I^{(s)}(0)=\frac{\hbar}{2e}\left(I^{(\uparrow)}(0)-I^{(\downarrow)}(0)\right)$ are the spin-current densities along the direction of $\mathbf{M}_2$ for the AF and FM configurations, respectively, and the dynamic polarization is defined as $P(\theta)=\frac{\left(I^{(\uparrow)}(\theta)-I^{(\downarrow)}(\theta)\right)}{\left(I^{(\uparrow)}(\theta)+I^{(\downarrow)}(\theta)\right)}$. This result is important because it reduces the calculation of $T_{||}$ simply to the evaluation of spin-current densities for the FM and AF configurations. As expected, the angular dependence of both $T_{\perp}$ and $T_{||}$ is found to be proportional to sin(θ), in contrast to the corresponding behavior in metallic spin valves. In order to confirm the above equation we display also in Fig. 4 the bias dependence of $\frac{\hbar}{2e}\frac{P(\pi)I(\pi)-P(0)I(0)}{2}$ (symbols associated with the right ordinate), where the agreement is excellent.

In order to elucidate the atomistic origin of the bias dependence of $T_{||}$, we plot in figure 7 the spin-current densities, versus bias for the AF and FM orientations, respectively for $\varepsilon_{\downarrow}$=2eV $. One can clearly see that $I^{(s)}(0)$ ($I^{(s)}(\pi)$) varies linearly (quadratic) with bias for V < 0.5 eV. For the FM and AF configurations the tunneling can be considered as the superposition of two independent spin channels. This different bias behavior can be understood on the basis of the Brinkman tunnel model[20] for asymmetric barriers, generalized so as to take into account both spin channels. In the FM configuration, the majority and minority electrons tunnel through a *symmetric* barrier (lower inset in Fig. 7) but with different barrier heights, for each spin channel. In this case, $\bar{\Phi}^{\uparrow}\neq\bar{\Phi}^{\downarrow}$ and $\Delta\Phi^{\uparrow}$=

$\Delta\Phi^{\downarrow}$=0. Thus, both $I^{\uparrow}(0)$ and $I^{\downarrow}(0)$ vary linearly with bias, and hence also $I^{(s)}(0)$. On the other hand, in the AF configuration (upper inset in Fig. 7), both spin channels tunnel through asymmetric barriers with the same average barrier height, but with barrier

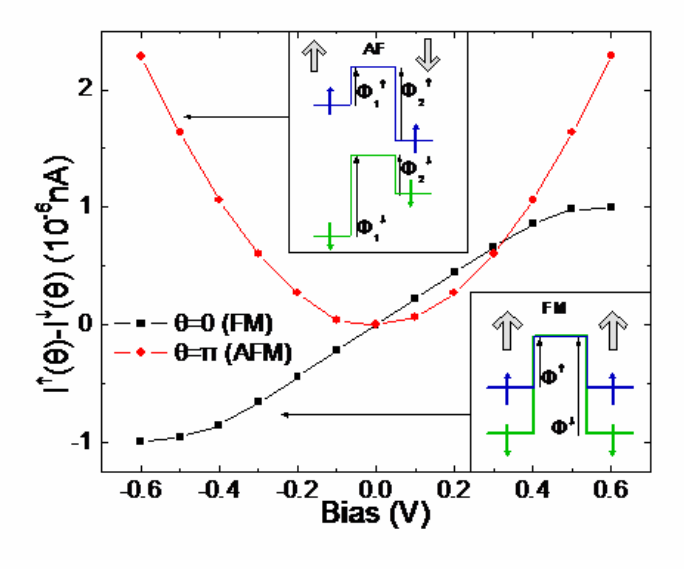

Figure 7 *Bias dependence of the spin-current density, for the FM (θ=0) and AF (θ=π) orientations, respectively. In the FM case the majority and minority electrons tunnel through a symmetric barrier (lower inset) with different barrier heights, Φ^{σ}. In the AF case (upper inset), the two spin channels tunnel through asymmetric barriers with the same average barrier height, $(\Phi^{\uparrow}+\Phi^{\downarrow})/2$, but with a barrier asymmetry, $\Delta\Phi^{\sigma}$, of opposite sign.*

asymmetry of opposite sign, $\Delta\Phi^{\uparrow}$= - $\Delta\Phi^{\downarrow}$. Hence, the linear bias dependence of $I^{\uparrow}(\pi)$-$I^{\downarrow}(\pi)$vanishes identically, and $I^{(s)}(\pi)$ exhibits a quadratic bias dependence.

Thus, the interplay between the linear and quadratic bias-dependence of $I^{(s)}(0)$ and $I^{(s)}(\pi)$, respectively, in the above equation is responsible for the non-monotonic dependence of with bias. The publications resulted from this research work are listed as Refs. 7-10 in Sec. IV.

4. Enhancing the Spin Torque in Double Barrier Magnetic Tunnel Junctions

Spintronics involve the exploitation of the quantum-mechanical spin degree of freedom to provide new functionalities beyond conventional electronics. One effect that has its roots on the electron's spin, is the torque exerted on the magnetization of a nanometer-scale free ferromagnet (FM) by a spin-polarized current, originating from a preceding non-collinear pinned FM[13-16]. This torque can be decomposed into a field-like and a spin-transfer component, both orthogonal to the magnetic moment of the free FM, but with different influence on its dynamics. At sufficiently high current densities, the spin-transfer torque leads to current-induced magnetization switching (CIMS). Reduction of the high critical current for CIMS is necessary for spin-transfer controlled magnetic memories.

Double-barrier magnetic tunnel junctions (DBMTJ) consist of a central metallic layer between two insulating barriers and two FM electrodes. The tunneling magnetoresistance (TMR) can be dramatically enhanced in collinear DBMTJ by the presence of quantum well states (QWS) under appropriate resonant conditions. While the physics in *collinear* DBMTJ has been studied extensively, the effect of spin-polarized QWS (SPQWS) on the spin-torque in *non-collinear* DBMTJ remains an unexplored area thus far.

The objective of this work is to present for the first time a study of the effect of SPQWS on both the spin-transfer and field-like components of the spin torque under external bias. The calculations are based on the tight-binding method and the non-equilibrium Keldysh

formalism. We predict that both components of the local spin torque can be dramatically enhanced when majority and minority QWS energies of different quantum numbers are in close proximity and lie within the bias window. It should be emphasized that the local-spin-torque enhancement is not associated with an enhancement of the corresponding spin-polarized currents. The low-temperature bias dependence of the local spin-transfer torque, exhibits a switch-on and switch-off step-like behavior when the SPQWS enter the bias window or exit the energy band, respectively, similar to that of the spin-polarized currents. On the other hand, $T_{i\perp}$ changes sign between the majority and minority switch-on values of bias. We demonstrate that the bias behavior of $T_{i,\parallel}$ and $T_{i\perp}$ can be derived analytically using a single-site central FM region. The net $T_{\perp}$, pertinent to the non-equilibrium interlayer exchange coupling exhibits an anomalous angular behavior due to the interplay of the bilinear and bi-quadratic effective exchange couplings which have different bias behavior.

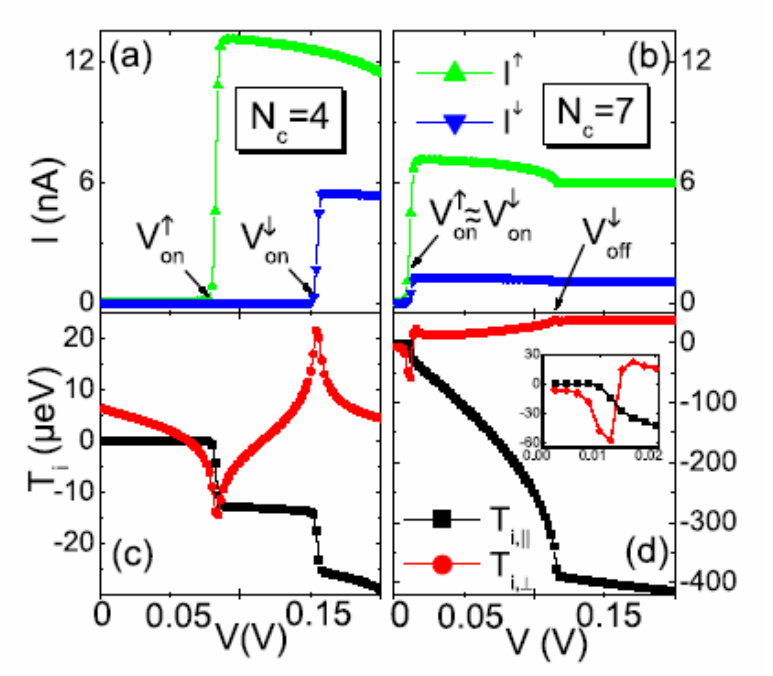

Figure 8 *Low-temperature (T=5K) bias dependence of the majority (green symbols) and minority (blue symbols) currents in the central FM for (a) N_c=4 AS and (b) N_c=7, respectively, and for $\theta = \pi/2$. Bias dependence of $T_{i||}$ (black symbols) and $T_{i\perp}$ (red symbols) on the first site in the central FM, for (c) N_c = 4 AS and (d) Nc=7 AS. The bias V^{σ}_{on} denote the switch-on bias.*

In Figs. 8a and 8b, we display the low-temperature (T = 5K) bias dependence of the spin-polarized currents, I↑ and I↓, for N_c = 4 atomic sites (AS) and N_c=7 AS, respectively, and for $\theta = \pi/2$. The spin-polarized currents switch on at $V^{\sigma}_{on} = 2|E(n^{\sigma})-E_F|$, when the n^{σ} QWS enters the bias energy window. For N_c=7 AS, the switch on for both spin-polarized currents occur at about the same bias. Both currents decrease with increasing bias because the density of states of the minority band in the leads at $E(n^{\sigma})$ decreases. At the critical bias are shifted below the bottom of the minority band of the lead, and hence the minority contribution to the spin-polarized currents is switched off. The publications resulted from this research work are listed as Ref. 11 in Sec. IV.

5. Interplay of Electron-Electron and Electron-phonon coupling in strongly correlated electron nanoclusters

Many condensed matter phenomena require a detailed understanding of the interplay between the electron-electron interactions (EEI) and electron-phonon interactions (EPI). Notable examples are high-temperature superconductors,[21] heavy fermions, Kondo, and valence-fluctuation systems,[22] and superconducting doped fullerenes,[23] among others.

Physics at the nanoscale provides a new and challenging stage to investigate such an interplay: Due to the spatial confinement, in nanosystems EEI can be hardly ignored, whilst EPI often act as a primary source of dissipation and decoherence of electronic processes. A case in point is single-molecular strongly correlated quantum dots.[24] In contrast to semiconductor quantum dots, which are quite rigid in space, molecules involved in the electron tunneling process naturally possess the vibrational degrees of freedom which may play a prominent role in electron transport. Another significant example is provided by small (open) systems relevant to spin-based quantum computation technology, where tailoring the magnetic properties (and their deterioration via EPI and EEI) is required for entanglement realization and processing.

The interplay between the EEI and EPI remains largely an open problem because there are no generally reliable theoretical methods to describe the electron-phonon interaction in strongly correlated electron systems. For weakly correlated electrons and EPI we have the successful Migdal-Eliashberg theory.[25] However, in many situations of interest the EEI are important, a Fermi liquid description may not be appropriate, and the relevant expansion parameter is unclear. One such case, relevant to this work, is heavy Fermion systems, where localized levels with strong local EEI hybridize with weakly correlated bands.

The purpose of this work is to study strongly correlated Anderson nanoclusters with one and two impurities in the charge-fluctuation regime and explored the role of (weak to strong) EPI, using exact diagonalization calculations. These systems are pertinent to quantum dots and quantum computation. We find that: i) The EPI induce a downwards shift of the impurity level, whilst reducing at the same time the "bare" interaction U; ii) for impurity levels initially in the mixed valence regime, such a renormalization and screening drives the single-impurity Anderson Hamiltonian first towards the symmetric regime, enhancing the local moment, (LM) ; further increase of the EPI leads to the double occupancy of the impurity level; iii) Consequently, the LM reaches its maximum value at the symmetric regime; iv) for two impurities in the mixed valence regime, the system can exhibit magnetic order in the ground state, depending on the separation between the impurities and the value of the EPI. Consequently, the EPI affects the competition between Kondo and RKKY correlation, producing in some cases reentrant ferromagnetic phases.

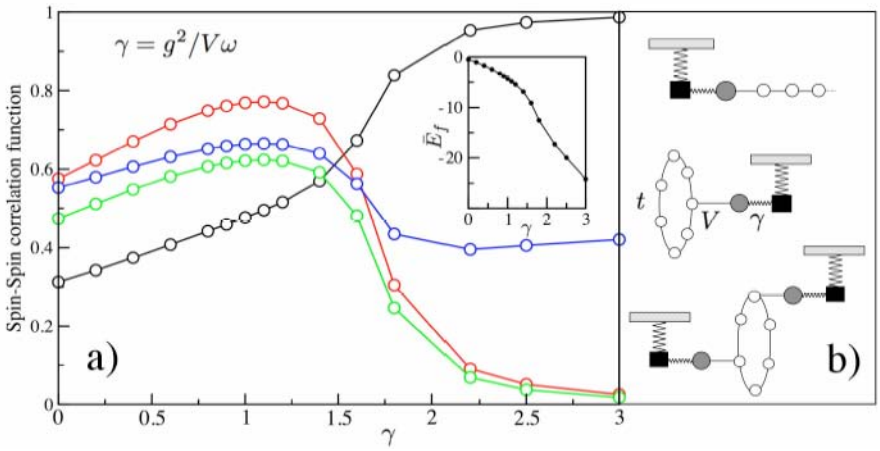

Figure 9 Main: *Spin-Spin correlation functions and average occupation at the impurity site as a function of the electron-phonon coupling γ : The black, red, green and blue curves refer to average f-occupation number $<n_f>$, the average f local moment $<\mu^2_f>$, the on-site f-electron conduction-electron spin correlation function, $<S_f S_c>$,and the on-site average conduction electron $<S^2_c>$, respectively.* ***Left inset:*** *average level shift as function of the EPI strength. Fig.1b): Cluster geometries used for the one- (top, medium) and two-impurity cases.*

In this report, we present results only for the case of the single impurity. We have used two different cluster geometries, i.e., open chains and rings, as shown in Fig. 9, right panel (top and medium geometries). Upon increasing the EPI, the local moment rises to a maximum value around γ=1.1, and then decreases monotonically to zero. The EPI thus provide a region of enhancement of the LM, compared to the γ=0 case. It is useful to consider the behavior of the average impurity occupation $<n_f>$ (black curve): its value increases monotonically with electron-phonon coupling, saturating to the value of $<n_f>=1$ for large EPI. The enhancement of the local moment reflects also in the behavior of the on-site f-electron conduction-electron spin correlation function, $<S_f S_c>$ (green curve), which follows quite closely that of average f local moment$< \mu^2_f >$,, and which is an indication of Kondo correlations. The publications resulted from this research work are listed as Refs. 12 in Sec. IV.

III. Scientific Personnel

The following scientific personnel were involved in the research program during the 2003 -2007 grant period and were supported by the US Army grant award: Prof. Nicholas Kioussis (PI), and Drs. Y. Liu and Z. Chen (postdoctoral fellows). Matching funds from the University have enabled support of a Ph.D. graduate student, Mr. Ioannis Theodonis, who has been carrying out the spin transport calculations described in Secs. 4 and 5.

IV. Publications

1. *An improved multiscale modeling approach for metals*, Y. Liu, Gang Lu, Zhengzheng Chen, and Nicholas Kioussis, Model. and Simulation in Materials Science and Engineering, **15,** 275 (2007).
2. Local Chemistry Effect on Dislocation Mobility: Dual Nature of Solutes, Z. Chen, N. Kioussis, and G. Lu, to be submitted to Phys. Rev. Lett. (February 2008).
3. N. M. Ghoniem and N. Kioussis, *Hierarchial Models of Nanomechanics and Micromechanics*, Chap. 64, Handbook of Theoretical Computational Nanotechnology, Ed. M. Rieth and W. Schommers, Vol. **1**, pp. 1-97 (2005).
4. *Non-singular descriptions of dislocation cores: a hybrid ab initio continuum approach*, S. Banerjee, N. M. Ghoniem, G. Lu, N. Kioussis, Phil. Mag. B **87**, 4131 – 4150 (2007).
5. *Dislocation threading across Cu/Ni interface: A hybrid atomistic-continuum approach*, M. Shehadeh, G. Lu, N. Kioussis, S. Banerjee, and N. Ghoniem, Phil. Mag. **87**, 1513 (2007).
6. *Multiplane-induced widening of stacking faults in fcc metals*, M. Shehadeh, G. Lu, N. Kioussis, and N. Ghoniem, Appl. Phys. Lett. **91**, 171905 (2007).
7. *Evolution of Magnetism of Cr nanoclusters on Au (111) surface: First principles electronic structure calculations*, H. Gotsis, N. Kioussis, and D. Papaconstantopoulos, , Phys. Rev. B. **73**, 014436 (2006).
8. *Spin-polarized current-induced torque in magnetic tunnel junctions*, A. Kalitsov, I. Theodonis, N. Kioussis, M. Chshiev, and W. Bulter, J. Appl. Phys. **99,** 08G501 (2006).

9. *Anomalous Bias Dependence of spin torques in magnetic tunnel junctions,* I. Theodonis, N. Kioussis, A. Kalitsov, M. Chshiev, and W. H. Butler, Phys. Rev. Lett. **97**, 237205 (2006).
10. *Spin transfer torque in double barrier magnetic tunnel junctions, I.* Theodonis, A. Kalitsov, and N. Kioussis, J. Magn. and Magn. Mater. **310**, 2043 (2007).
11. *Enhancing spin-transfer torque through the proximity of quantum well states,* I. Theodonis, A. Kalitsov, and N. Kioussis, Phys. Rev. B **76**, 224406 (2007).
12. *Electron-Electron versus Electron-Phonon Interactions in Anderson-Holstein Nanoclusters,* C. Verdozzi and N. Kioussis, to be submitted to Phys. Rev. B (2008).

V. References

1. E. B. Tadmor, M. Ortiz, and R. Phillips, Philos. Mag. **A 73,** 1529 (1996).
2. N. Choly, G. Lu, W. E, and E. Kaxiras, Phys. Rev. **B 71**, 094101 (2005).
3. G. Lu, E. B. Tadmor, and E. Kaxiras, Phys. Rev. **B 73**, 024108 (2006).
4. G. Fantozzi, C. Esnouf, W. Benoit, and I.G. Ritchie, Prog. Mater. Sci. **27**, 311 (1982).
5. F.R.N. Nabarro, Philos. Mag. **A 75**, 703 (1997).
6. A. Misra, J.P. Hirth and H. Kung, Phil. Mag. *A*, **82,** 2935 (2002).
7. A. Misra and H. Kung, Advanced Engineering Materials, **3,** 217 (2001).
8. R. G. Hoagland, T. E. Mitchell, J. P. Hirth, and H. Kung,. Phil. Mag, **82,** 643 (2002).
9. I. Rao, and P. M. Hazzledine, Phil. Mag. A, **80,** 2011 (2000).
10. G. Lu, N. Kioussis, V. Bulatov, and E. Kaxiras, Physical Review B, **62**(5), 3099 (2000).
11. G. Lu, V. Bulatov, and N. Kioussis, Physical Review B, **66,** 144103 (2002).
12. G. Lu, Q. Zhang, N. Kioussis, and E. Kaxiras, Phys. Rev. Lett. **87**, (2001).
13. J.C. Slonczewski, J. Magn. Magn. Matter. **159**, L1 (1996).
14. L. Berger, Phys. Rev. **B 54,** 9353 (1996).
15. J.C. Slonczewski, Phys. Rev. **B 39**, 6995 (1989).
16. J.C. Slonczewski, Phys. Rev. **B 71**, 024411 (2005).
17. E.B. Myers, D.C. Ralph, J.A. Kattine, R.N. Louie, R.A. Buhrman, Science **285**, 867 (1999).
18. G. D. Fuchs et al, Phys. Rev. Lett. **96**, 186603 (2006).
19. S.P. Parkin, K.P. Roche, M.G. Samant, P.M. Rice, R.B. Beyers, R.E. Scheurlein, E.J. O'Sullivan, S.L. Brown, J. Bucchigano, D.W. Abraham, Y. Lu, M.Rooks, P.L. Troulloud, R.A. Wanner, and W.J. Gallagher, J. Appl. Phys. **85**, 5828 (1999).
20. W. F. Brinkman, R. C. Dynes, and J. M. Rowell, J. Appl. Phys. **41**, 1915 (1970).
21. A. Lanzara, P. V. Bogdanov, X. J. Zhou, S. A. Kellar, D. L. Feng, E. D. Lu, T. Yoshida, H. Eisaki, A. Fujimori, K. Kishio, J.-I. Shimoyama, T. Noda, S. Uchida, Z. Hussain, and Z.-X. Shen, Nature (London) **412**, 510 (2001).
22. J. C. Lashley, J. Singleton, A. Migliori, J. B. Betts, R. A. Fisher, J. L. Smith, and R. J. McQueeney, Phys. Rev. Lett. **91**, 205901 (2003).
23. O. Gunnarsson, Rev. Mod. Phys. **69,** 575–606 (1997).
24. P. S. Cornaglia, H. Ness, and D. R. Grempel Phys. Rev. Lett. **93,** 147201 (2004); P. S. Cornaglia, D. R. Grempel, and H. Ness, Phys. Rev. B **71**, 075320 (2005).
25. A.B. Migdal, Sov. Phys. JETP **7,** 996 (1958); G.M. Eliashberg, *ibid.* **11**, 696 (1960).